



ISSN NO. 2320-5407

Journal homepage: <http://www.journalijar.com>

INTERNATIONAL JOURNAL  
OF ADVANCED RESEARCH

## RESEARCH ARTICLE

## Cobalt (II) complexes containing bisimine ligands as models for catechol oxidase and Phenoxazinone synthase

Abd El-Motaleb M. Ramadan,<sup>1</sup> Shaban Youssef,<sup>2</sup> Hatem Eissa<sup>3\*</sup><sup>1</sup> Professor of Inorganic Chemistry, Faculty of Science, Kafr El-Sheikh University, Kafr El-Sheikh, Egypt.<sup>2</sup> Associate Professor of Inorganic Chemistry, Faculty of Science, Kafr El-Sheikh University, Kafr El-Sheikh, Egypt.<sup>3</sup> PhD graduate Student, Chemistry Department, Faculty of Education, Kafr El-Sheikh University, Kafr El-Sheikh, Egypt.

### Manuscript Info

#### Manuscript History:

Received: 12 June 2014  
Final Accepted: 25 July 2014  
Published Online: August 2014

#### Key words:

Biomimetic, Catechol oxidase,  
Phenoxazinone synthase, cobalt(II)  
models.

#### \*Corresponding Author

Abd El-Motaleb M.  
Ramadan

### Abstract

The oxidation of 4-*tert*-butylcatechol (TBC) and 2-aminophenol (OAP) by molecular oxygen in the presence of a catalytic amount of cobalt(II) complexes was studied. The catecholase biomimetic catalytic activity of the cobalt(II) complexes has been determined spectrophotometrically by monitoring the oxidative transformation of 4-*tert*-butylcatechol and 2-aminophenol to the corresponding light absorbing 4-*tert*-butylquinone (Q) and 2-amino-3H-phenoxazin-3-one, respectively. The rate of the catalytic oxidation reaction was investigated and correlated with the catalyst structure, time, concentration of catalyst and substrate and finally solvent effects. Addition of Et<sub>3</sub>N, CH<sub>3</sub>CN and thiourea showed a dramatic effect on the rate of oxidation reaction. Kinetic investigations demonstrate that the rate of oxidation reaction has a first order dependence with respect to the catalyst and substrate concentration and obeying Lineweaver-Burk Kinetics. It was shown that the catalytic activity depends on the coordination environment of the catalyst created by the ligand.

Copy Right, IJAR, 2014. All rights reserved

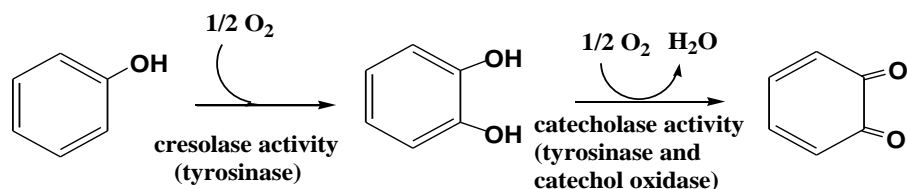
### Introduction

The transition metal compounds can act as catalysts in many organic oxidation reactions (Sheldon et al., 1981). Copper compounds especially, occupy a major place in oxidation chemistry due to their abundance in natural and biological media (Kitajima et al., 1994). Because of its occurrence in many natural enzymatic processes, the interaction of molecular oxygen with copper in its different oxidation states was also a subject of numerous investigations (Karlin et al., 1983).

Based on their spectroscopic characteristics, three types of active site are distinguished in copper proteins (Malmstrom et al., 1982). Proteins with type-3 copper centers can serve either as oxygenase / oxidase enzymes or as dioxygen transport proteins (Solomon et al., 1996). An example of an oxygen carrier protein is hemocyanin (HC), a well-known member of this class of copper proteins. HCs can be divided into two classes depending on their biological source: the arthropodan (e.g., lobsters and spiders) and the molluscan (e.g., octopus and snails) hemocyanins. These have different subunit organizations and only a weak evolutionary relationship (van Holde et al., 1995).

Catechol oxidase (CO), also known as *o*-diphenoloxidase, is a less well known member of the type-3 copper proteins (Solomon et al., 1996). The official nomenclature is 1,2-benzenediol: oxygen oxidoreductase,

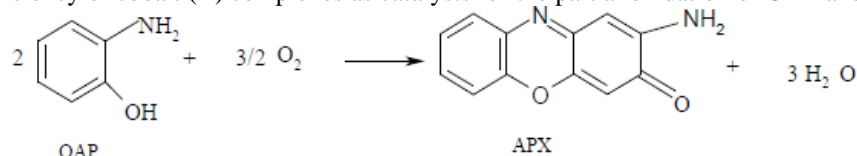
indicating that dioxygen is the second substrate. CO catalyzes exclusively the oxidation of catechols (i.e., *o*-diphenols) to the corresponding *o*-quinones (called catecholase activity, Scheme 1).



**Scheme 1.** Reaction pathway of the oxygenation and oxidation catalyzed by TYR and CO.

Catechol oxidase catalyzes the oxidation of *o*-diphenols (catechols) to the quinones through four-electron reduction of dioxygen to water and Krebs and co-workers proposed a mechanism for the catalytic process, based on biochemical, (Solomon et al., 1996, Wilcox et al., 1985) spectroscopic (Eicken et al., 1998) and structural (Klabunde et al., 1998) data.

The oxidation of 2-aminophenol (OAP) to 2-aminophenoxazin-3-one (APX) in the presence of tyrosinase, a copper containing mono oxygenase, is a well-known reaction (Toussaint et al., 1987, Barry et al., 1989) and used as model for the biosynthesis of the powerful antineoplastic agent, actinomycin D (Frei et al., 1987). The overall stoichiometric equation for OAP oxidation is shown in Scheme 2. Our work provides a comparative study concerning the efficiency of cobalt (II) complexes as catalysts for the partial oxidation of OAP and TBC.



**Scheme.2:** Overall equation of 2-aminophenol oxidation to 2-aminophenoxazinone.

## 2. Experimental Part

### 2.1. Materials and general methods:

Unless noted otherwise, all procedures were carried using Schlenk techniques. Spectra were recorded on the following instruments: IR (KBr) discs or CaF<sub>2</sub> cuvettes, solvent bands were compensated): FT-IR Bruker Vector 22 spectrometer, Germany in the range 400-4000 cm<sup>-1</sup>. Around 1.0 mg of a substance in the form of fine powder was mixed and ground well with about 100 mg of a spectroscopically pure KBr powder (Merck). The mixture was pressed then in a special disc under vacuum at pressure of about 150 Kg/cm<sup>-1</sup> using a hydraulic press. The disc produced was 1.2 cm in diameter and of about 0.7 mm thickness. Spectra were recorded at 25 °C; -Elemental analyses: Elementary III CHNS Analyzer, Germany. Thermogravimetric analysis was performed using Shimadzu Stand-Alone Thermal Analyzer Instruments (TGA 50H) Japan. About 5 mg of pure sample was subjected to dynamic TGA scans at a heating rate 10 °C/min in the temperature range of ambient to 900 °C under a dynamic atmosphere of dry nitrogen gas (flow rate = 10 ml/min). The TGA curves were analyzed as percentage weight loss as a function of temperature. The dehydration and composition steps were identified using a derivative of the TGA (D-TGA) curves. All UV-visible absorptions of coordinated compounds in solution state were recorded by UV-2040 spectrophotometer Shimadzu, Japan and quartz cuvette. All chemicals used in the present study were analytical grade chemicals and were used as received without further purification. CoCl<sub>2</sub>·6H<sub>2</sub>O obtained from Wako-Japan, 2,6-pyridine dimethanol and selenium dioxide from Aldrich, 1,3-diamino-2-hydroxy propane and 4-methyl-1,2-phenyldiamine from Sigma-Aldrich.

### 2.2. Synthesis.

**2.2.1. 2,6-Pyridine dialdehyde:** 2,6-pyridine dimethanol (0.072 mol) and selenium dioxide (0.072 mol) were dissolved in dioxane (300 ml), the mixture was turned off orange red at 70 °C and brown at 100 °C. After heating at reflux 5 h, the solution was filtered and the solvent was removed by evaporation. The crude product was recrystallized from chloroform-light petroleum (p.b. 40-60 °C) to give the brown product. Yield (70 %), M.p. (124 °C); IR (KBr, cm<sup>-1</sup>) in figure 1: 3081 (ν, C-H<sub>aromatic</sub>), 2870 (ν, C-H<sub>aliphatic</sub>), 2861, 1712(ν, C=O), 1452 (ν, pyridine).

**2.2.2. Synthesis of [Co<sub>2</sub>L<sup>1</sup>Cl<sub>4</sub>] · 2H<sub>2</sub>O (1):** 2,6-pyridine dicarbaldehyde (0.0011 mol) was dissolved in 10 ml ethanol, CoCl<sub>2</sub>·6H<sub>2</sub>O (0.0022 mol) was added and the mixture was stirred for 1.5 h. 1,3-diamino-2-hydroxy propane (0.0022 mol) was added. The mixture was stirred over night after that, the mixture was filtered and washed

with diethyl ether to give a dark green solid. Yield (69 %), M.p. (>300 °C); IR (KBr,  $\text{cm}^{-1}$ ): 3413-3212 (*b*, N-H), 3098 ( $\nu$ , C-H<sub>aromatic</sub>), 2928 ( $\nu$ , C-H<sub>aliphatic</sub>), 1616 ( $\nu$ , C=N), 1452( $\nu$ , pyridine); Elemental analysis: Found. C 27.35, H 4.91; calcd C 27.15, H 4.38.

**2.2.3. Synthesis of  $[\text{Co}_2\text{L}^2\text{Cl}_4] \cdot 3\text{H}_2\text{O}$  (2):**  $\text{CoCl}_2 \cdot 6\text{H}_2\text{O}$  (0.0022 mol) was added to a solution of 2,6-pyridine-dicarbaldehyde (0.0011 mol) in 10 ml ethanol and the mixture was stirred for 1h. 4-methyl-1,2-phenyldiamine (0.0022 mol) was then added and the mixture was refluxed for 5h. The mixture was filtered off and washed with diethyl ether to give a brown solid. Yield (54 %), M.p. (192 °C); IR(KBr,  $\text{cm}^{-1}$ ): 3424(*b*, N-H), 3080( $\nu$ , C-H<sub>aromatic</sub>), 2860 ( $\nu$ , C-H<sub>aliphatic</sub>), 1614 ( $\nu$ , C=N), 1452( $\nu$ , pyridine); Elemental analysis: Found C 37.81, H 4.30; calcd, C 38.44, H 3.99.

### 2.1. Catecholase assays

Biomimetic activity was measured against 4-*tert*-butylcatechole (TBC) and 2-aminophenol (OAP). Kinetic assays were conducted in DMF (saturated with  $\text{O}_2$ ) at 298 K and formation of product was monitored around 400 nm ( $\epsilon = 1,900 \text{ M}^{-1} \text{ cm}^{-1}$ ). Under these conditions no formation of quinone was observed in the absence of the cobalt complexes.

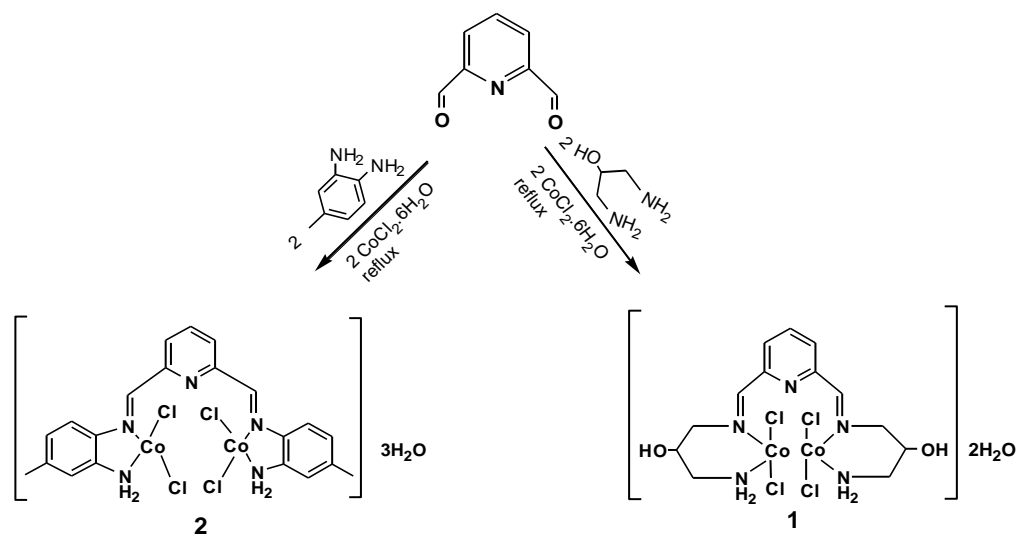
## 3. Results and discussions

The cobalt (II) complexes,  $[\text{Co}_2\text{L}^1\text{Cl}_4] \cdot 2\text{H}_2\text{O}$  (**1**) and  $[\text{Co}_2\text{L}^2\text{Cl}_4] \cdot 3\text{H}_2\text{O}$  (**2**), were prepared by reacting of 2,6-pyridine dicarbaldehyde (pdc), cobalt(II) chloride with the appropriate diamine ligands. (Scheme 3). The addition of diethyl ether to the reaction solution afforded colored crystals. IR (KBr) spectra of both complexes show the disappearance of the  $\nu$  (C=O) peak and the appearance of the imine  $\nu$ (C=N) peak indicating the condensation and the formation of imine species. Complex **1** exhibits other peaks at  $\nu$ (3212)  $\text{cm}^{-1}$  and  $\nu$ (3413)  $\text{cm}^{-1}$  attributed to  $\nu$ (N-H) (Figure 1). Complex **2** exhibits peaks at  $\nu$ (3424)  $\text{cm}^{-1}$  attributed to  $\nu$ (N-H)  $\text{cm}^{-1}$  (Figure 1).

Conductivity measurements of complexes **1** and **2** are carried out in DMF solution of  $10^{-3}$  mmol and exhibit values of 39 and 33  $\Omega^{-1}$  for **1** and **2** respectively. These values are in agreement of the structures given in (scheme 3). This gives more evidence for absence of counter anion for these complexes.

The TGA curve of complex **1** (Figure 2) shows decomposition steps within the temperature range 50-900 °C. The first step of the decomposition within the temperature range 40-90°C (table 1) corresponded to the loss of two lattice water molecules with a mass loss of 6.75 % (calcd. 6.26 %). The second step within the temperature range 90-430 °C corresponded to the loss of coordinated four chloride atoms with a mass loss of 25.02 % (calcd. 24.69 %). The last steps of the decomposition within the temperature range 430-650 °C corresponded to the loss of the organic part of the complex with a mass loss of 42.55 % (calcd 42.98 %). The final residue corresponded to (CoO) metal with a mass of 20.19 % (calcd 20.50 %).

The TGA curve of complex **2** (Figure 3) shows decomposition steps within the temperature range 50-900 °C. The first step of the decomposition within the temperature range 40-160°C (table 1) corresponded to the loss of three lattice water molecules with a mass loss of 8.93 % (calcd. 8.22 %). The second step within the temperature range 160-430 °C corresponded to the loss of coordinated four chloride atoms with a mass loss of 22.04 % (calcd. 21.64 %). The last steps of the decomposition within the temperature range 430-570 °C corresponded to the loss of the organic part of the complex with a mass loss of 47.65 % (calcd 47.30 %). The final residue corresponded to (CoO) metal with a mass of 16.81 % (calcd 17.96 %).



**Scheme 3.** Reaction of 2,6-pyridine dicarbaldehyde (*pdc*) with appropriate diamine to give cobalt complexes **1** and **2**.

**Table 1 .** Thermo gravimetric analysis data of cobalt(II) complexes **1** and **2**.

Complex	Temperature range °C	Weight loss Found (calcd)	Species formed
<b>1</b>	40 – 90	6.75 (6.26)	[Co <sub>2</sub> L <sup>1</sup> CL <sub>4</sub> ]
	90 – 430	25.02 (24.69)	[Co <sub>2</sub> L <sup>1</sup> ]
	430 – 650	42.55 (42.98)	CoO
<b>2</b>	40 – 160	8.93 (8.22)	[Co <sub>2</sub> L <sup>1</sup> CL <sub>4</sub> ]
	160 – 430	22.04 (21.64)	[Co <sub>2</sub> L <sup>1</sup> ]
	430 – 570	47.65 (47.30)	CoO

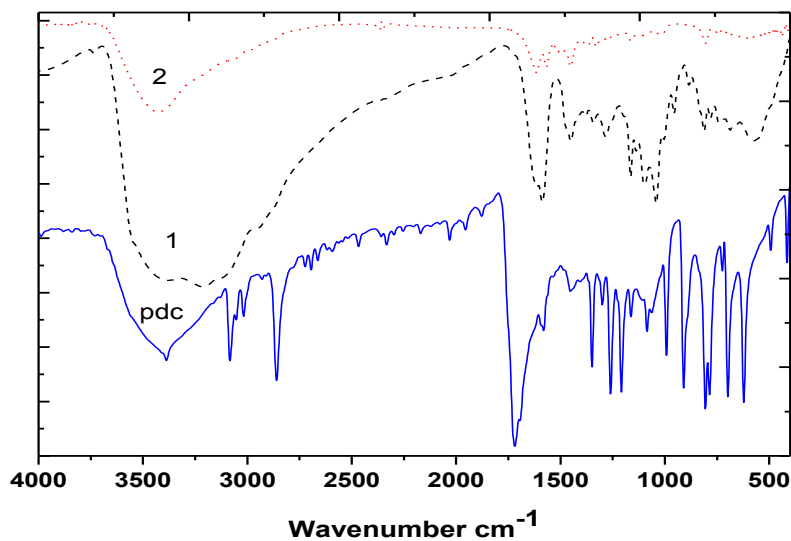


**Fig 1:** IR (KBr) spectra of *pdc*, **1** and **2**.

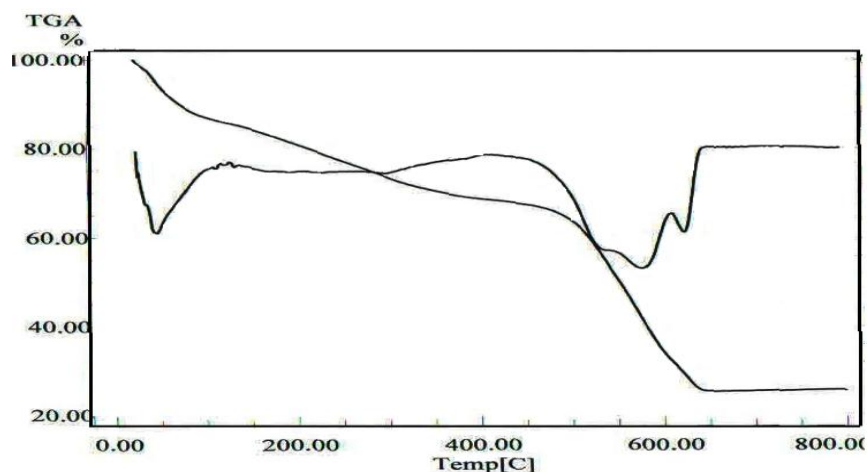


Fig 2: TGA and DTG curves for complex 1.

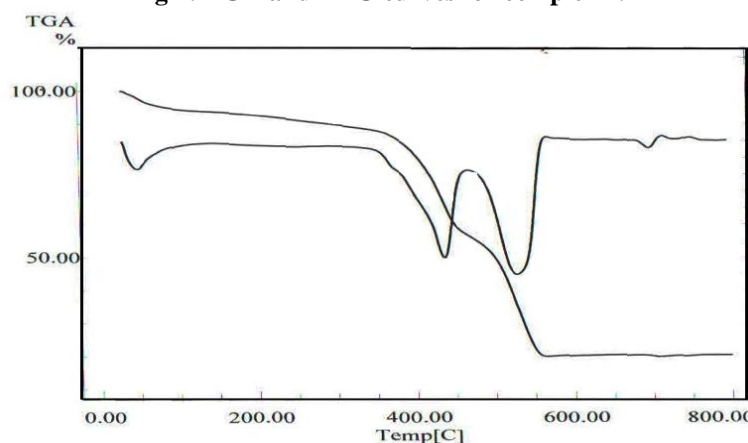


Fig 3: TGA and DTG curves for complex 2

#### Kinetic study for series of cobalt complexes with TBC.

Kinetic study for series of cobalt complexes with various ligands, it was first necessary to estimate approximately the ability of the complexes to oxidize 4-*tert*-butylcatechol. For this purpose, 0.1 mmol L<sup>-1</sup> solutions of **1** and **2** in DMF were treated with 100 mmol L<sup>-1</sup> of 4-*tert*-butylcatechol in the presence of air. The course of the reaction was followed by UV-Vis spectroscopy at  $\lambda = 400$  nm over 32 min. The results indicate that the reactivity of **2** is higher than **1**, and can be expressed in turnover numbers indicated in table 3. The rate of oxidation of 4-*tert*-butylcatechol is depended on the nature of the ligand attached to the metal ion. Two factors are considered to account for the difference in reactivities of these complexes. The redox potential of the cobalt ion and the positive ligand influence are considered to be affected by the coordination environment, the behavior of the complexes can be rationalized by means of correlation between the nature of the coordinated axial counter anion and the catecholase biomimetic and catalytic activity.

#### Dependence of rate on 4-*tert*-butylcatechol concentration.

To determine the dependence of the observed reactions on the substrate concentration, solutions of **1** were treated with different concentrations of TBC in methanol. TBC concentration spanned the range 0.04 – 0.12 M and the catalyst concentration was  $2 \times 10^{-4}$  M. TBC solution was prepared directly before use to minimize its oxidation during storage. TBC solution 0.5 cm<sup>3</sup> was added to a solution of cobalt complex in cell of an appropriated concentration thermostated at 25 °C for at least 24 min. During the kinetic run, the reaction cell was not covered in

order to allow the solution to be continually exposed to air. The pH of the solution determined at the beginning and at the end of the kinetic run. Oxidation of TBC was followed spectrophotometrically by monitoring the formation of 4-*tert*-butylquinone, using a Shimadzu-240 spectrophotometer at  $\lambda = 400$  nm. Absorbance vs time relation for determination of the rate of the reaction ( $v_0$ ) is shown in figure 4.

The rate-determining step was found to change with the substrate to complex ratio. The Lineweaver–Burk treatment gives  $K_M = 0.04 \text{ M s}^{-1}$  and  $V_{\max} = 0.24 \text{ M s}^{-1}$ . This behavior indicates the presence of equilibrium in the rate-determining step (Figure 5).

#### Dependence of rate on catalyst concentration.

For determining the dependence of the observed reactions on the catalyst concentration, solutions of TBC were treated with different concentrations of **1** in methanol. Catalyst concentration spanned the range  $4 \times 10^{-5} - 2.4 \times 10^{-4} \text{ M}$  and the substrate concentration was  $4 \times 10^{-2} \text{ M}$ . TBC solution was prepared directly before use to minimize its oxidation during storage. The reaction was performed at  $25^\circ \text{C}$  for at least 24 min. During the kinetic run, the reaction cell was not covered in order to allow the solution to be continually exposed to air. The pH of the solution determined at the beginning and at the end of the kinetic run. Oxidation of TBC was followed spectrophotometrically by monitoring the formation of 4-*tert*-butylquinone, using a Shimadzu-240 spectrophotometer at  $\lambda = 400$  nm. A relation between time and absorbance for determination of the rate of the reaction ( $v_0$ ) and relation between  $V_0$  and concentration of the catalyst illustrate that the rate with high concentration of catalyst is stable and reach the saturation condition is shown in figure 6.

#### Factors affect the catecholase activity.

##### a) Effect of Lewis – base (B).

Effect of Lewis – base (B) Addition of triethylamine ( $\text{Et}_3\text{N}$ ) showed a dramatic effect on the rate of oxidation. In Figure 7 shows the effect of adding  $\text{Et}_3\text{N}$  on the rate of oxidation of 4-*tert*-butylcatechol in the methanol solution where the concentrations of metal complex **1** and 4-*tert*-butylcatechol were held constant. It is observed that the rate of oxidation increases initially with addition of  $\text{Et}_3\text{N}$ . There are two factors, which account for the increase of  $V_0$  value on addition of  $\text{Et}_3\text{N}$ . The first is a kinetic factor; in methanol solution catechol is mainly present in the  $\text{H}_2\text{A}$  form. Due to the presence of Lewis-base in the reaction medium, 4-*tert*-butylcatechol may be predominantly present in the monoprotonated form (HA). The kinetic activity of HA is presumably the spark for initiation of the catalytic oxidation cycle. The second factor is a thermodynamic. It is obvious that excessive bond stability of a metal substrate or any reacting species is unfavorable for a catalytic process. The bond must be stable enough to exist but must also be susceptible to reiterate the concerted reaction. In the present study, a noticeable color change was observed on addition of  $\text{Et}_3\text{N}$  to the metal complex solution in methanol. Also, at high concentration of  $\text{Et}_3\text{N}$ , a brownish to green precipitate was formed in the presence of the metal complex. Accordingly, we propose that the Lewis base (B) coordinates to the central cobalt ion. Figure 8 shows the effect of  $\text{Et}_3\text{N}$  concentrations on the reaction rate in the presence of catalyst, where the rate increases initially with increasing the  $\text{Et}_3\text{N}$  concentration. It reaches a maximum at a certain concentration of  $\text{Et}_3\text{N}$  (0.025 ml) and then decreases. The drop after the maximum rate can be attributed to the precipitation of catalyst due to its coordination with  $\text{Et}_3\text{N}$ . At high concentration of  $\text{Et}_3\text{N}$ , the concentration of adduct species,  $[\text{Et}_3\text{N-complex}]$ , increases and catalyst precipitates. This reveals that the more reactive generated species,  $[\text{Et}_3\text{N-complex}]$ , adduct has lower solubility than that of the original complex.

##### b) Effect of thiourea (TU).

Effect of thiourea (TU) Addition showed a dramatic effect on the rate of oxidation. Figure 9 shows the effect of adding thiourea on the rate of oxidation of 4-*tert*-butylcatechol in the methanol solution where the concentrations of metal complex **1** and 4-*tert*-butylcatechol were held constant. It is observed that the absorbance of 4-*tert*-butylquinone decreased dramatically in the presence of TU so the rate of oxidation decreased with addition of TU.

#### Kinetic study of cobalt complexes with OAP.

The reactions between 2-aminophenol (OAP) and dioxygen in the presence of catalytic amount of cobalt complexes were performed in DMF solution and examined at  $25^\circ \text{C}$ ,  $0.1 \text{ mmol L}^{-1}$  solutions of complexes cobalt **1** and **2** in DMF were treated with  $100 \text{ mmol L}^{-1}$  of *o*-aminophenol in the presence of air. The course of the reaction was followed by UV-Vis spectroscopy at  $\lambda = 400$  nm over 32 min. The results indicate that the reactivity of **1** is higher than **2**, and can be expressed in turnover numbers as listed in table 3. The rate of oxidation of *o*-aminophenol is dependent on the nature of ligand. Two factors can be considered to account for the difference in reactivities of



these complexes. The redox potential of the cobalt ion and the positive ligand influence are considered to be affected by the coordination environment, the behavior of the complexes can be rationalized by means of correlation between the nature of the coordinated axial counter anion and the phenoxazinase biomimetic and catalytic activity.

#### Dependence of rate on *o*-aminophenol concentration.

To determine the dependence of the observed reactions on the substrate concentration, solutions of **1** were treated with different concentrations of APO in methanol. APO concentration spanned the range 0.02 – 0.12 M and the catalyst concentration was  $2 \times 10^{-4}$  M. APO solution was prepared directly before use to minimize its oxidation during storage. APO solution  $0.5 \text{ cm}^3$  was added to a solution of cobalt complexes in a cell of an appropriated concentration thermostated at  $25 \text{ }^\circ\text{C}$  for at least 24 min. During the kinetic runs, the reaction cell was not covered in order to allow the solution to be continually exposed to air. The pH of the solution determined at the beginning and at the end of the kinetic runs. Oxidation of APO was followed spectrophotometrically by monitoring the formation of 2-amino-3H-phenoxazin-3-one, using a Shimadzu-240 spectrophotometer at  $\lambda = 400 \text{ nm}$ . A relation between time and absorbance for determination of the rate of the reaction ( $v_0$ ) is shown in figure **10**.

The rate-determining step was found to change with the substrate to complex ratio. The Lineweaver-Burk model treatment gives  $K_M = 0.45 \text{ M s}^{-1}$  and  $V_{\max} = 1.92 \text{ M s}^{-1}$  (Figure **11**). It's clear that the values of  $K_M$  and  $V_{\max}$  are different than that found in catalysis of TBC.

#### Dependence of rate on catalyst concentration.

For determining the dependence of the observed reactions on the catalyst concentration, solutions of OAP were treated with different concentrations of complex **1** in methanol. Catalyst concentration spanned the range ( $4 \times 10^{-5} - 2.4 \times 10^{-4}$ ) M and the substrate concentration was  $4 \times 10^{-2}$  M. OAP solution was prepared directly before use to minimize its oxidation during storage. The reaction was performed at  $25 \text{ }^\circ\text{C}$  for at least 30 min. During the kinetic run, the reaction cell was not covered in order to allow the solution to be continually exposed to air. The pH of the solution determined at the beginning and at the end of the kinetic run. Oxidation of OAP was followed spectrophotometrically by monitoring the formation of 2-amino-3H-phenoxazin-3-one, using a Shimadzu-240 spectrophotometer at  $\lambda = 400 \text{ nm}$ . A relation between time and absorbance for determination of the rate of the reaction ( $v_0$ ) and relation between  $V_0$  and concentration of the catalyst illustrate that the rate with high concentrations of catalyst is stable at  $2 \times 10^{-4}$  M and reaches the saturation condition is shown in figure **12**.

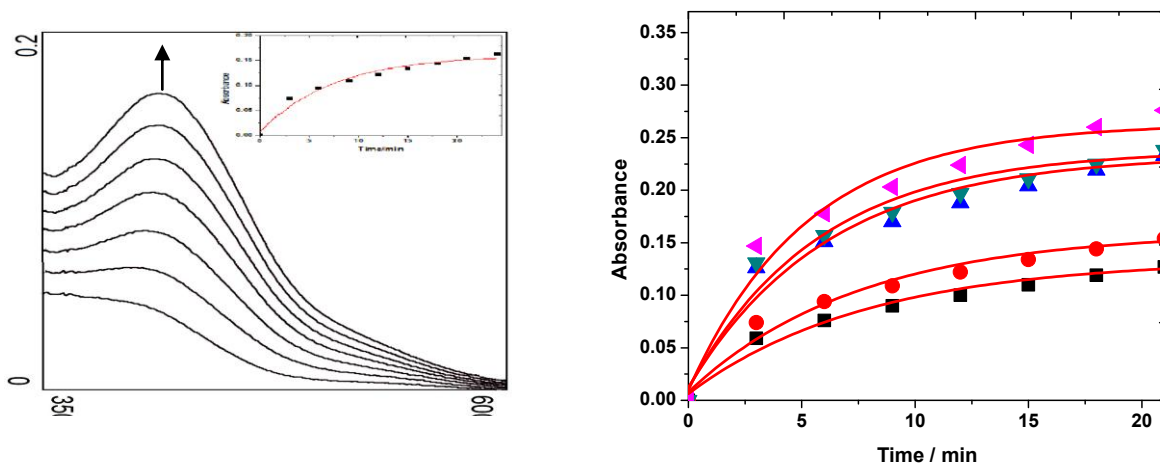
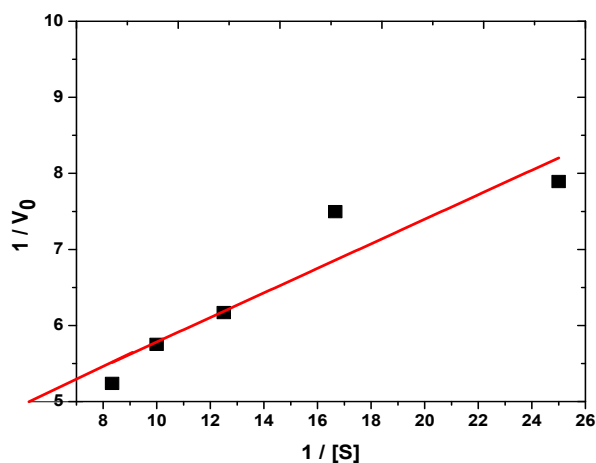
#### Factors affect the OAP activity.

##### a) Effect of Lewis – base (B).

Addition of Lewis – base (B) triethylamine ( $\text{Et}_3\text{N}$ ) showed a dramatic effect on the rate of oxidation. In figure **13** shows the effect of adding  $\text{Et}_3\text{N}$  on the rate of oxidation of *o*-aminophenol in the DMF solution where the concentrations of metal complex and *o*-aminophenol were held constant. It is observed that the rate of oxidation increases at the same concentrations initially with addition of  $\text{Et}_3\text{N}$ . There are two factors, which account for the increase of  $V_0$  value on addition of  $\text{Et}_3\text{N}$ . The first one is a kinetic factor; in DMF solution *o*-aminophenol is mainly present in the HA form. Due to the presence of Lewis-base in the reaction medium, *o*-aminophenol may be predominantly present in the monoprotonated form (HA). The kinetic activity of HA is presumably the spark for initiation of the catalytic oxidation cycle. The second factor is a thermodynamic. It is obvious that excessive bond stability of a metal substrate or any reacting species is unfavorable for a catalytic process. The bond must be stable enough to exist but must also be susceptible to reiterate the concerted reaction. In the present study, a noticeable color change was observed on addition of  $\text{Et}_3\text{N}$  to the metal complex solution in DMF. Also, at high concentration of  $\text{Et}_3\text{N}$ , a reddish precipitate was formed in the presence of the metal complex. Accordingly, we propose that the Lewis base (B) coordinates to the central cobalt(II) ion. In figure **14** shows the effect of  $\text{Et}_3\text{N}$  concentrations on the reaction rate in the presence of catalyst, where the rate increases initially with increasing the  $\text{Et}_3\text{N}$  concentration. It reaches a maximum at a certain concentration of  $\text{Et}_3\text{N}$  (0.075 ml) and then decreases but in the case of TBC reaches a maximum at a low concentration of  $\text{Et}_3\text{N}$  (0.025 ml). The drop after the maximum rate can be attributed to the precipitation of catalyst due to its coordination with  $\text{Et}_3\text{N}$ . At high concentration of  $\text{Et}_3\text{N}$ , the concentration of adducts species,  $[\text{Et}_3\text{N-complex}]$ , also increases and catalyst precipitates. This reveals that the more reactive generated species,  $[\text{Et}_3\text{N-complex}]$ , adduct has lower solubility than that of the original complex.

**Table 3. Kinetic data for the oxidation of 4-*tert*-butylcatechol and *o*-aminophenol by complexes 1 and 2 in DMF.**

Complex	Activity ( $\mu\text{mol mg}^{-1} \text{min}^{-1}$ ) 4- <i>tert</i> -butylcatechol	Activity ( $\mu\text{mol mg}^{-1} \text{min}^{-1}$ ) <i>o</i> -aminophenol
$[\text{Co}_2\text{L}^1\text{Cl}_4] \cdot 2\text{H}_2\text{O}$ (1)	0.225	0.41
$[\text{Co}_2\text{L}^2\text{Cl}_4] \cdot 3\text{H}_2\text{O}$ (2)	0.467	0.17

**Fig 4. (Left) UV spectra changes of the reaction of complex 1 =  $2 \times 10^{-4}$  M with different concentrations of 4-*tert*-butylcatechol in methanol; (right) relation between absorbance vs. time of the reaction at wave length of 400 nm.****Fig 5. Lineweaver-Burk plot of  $1/V_0$  vs  $1/[S]$  concentrations with range 0.04 - 0.12 M for complex 1 for determining  $K_M$  and  $V_{\max}$  values.**



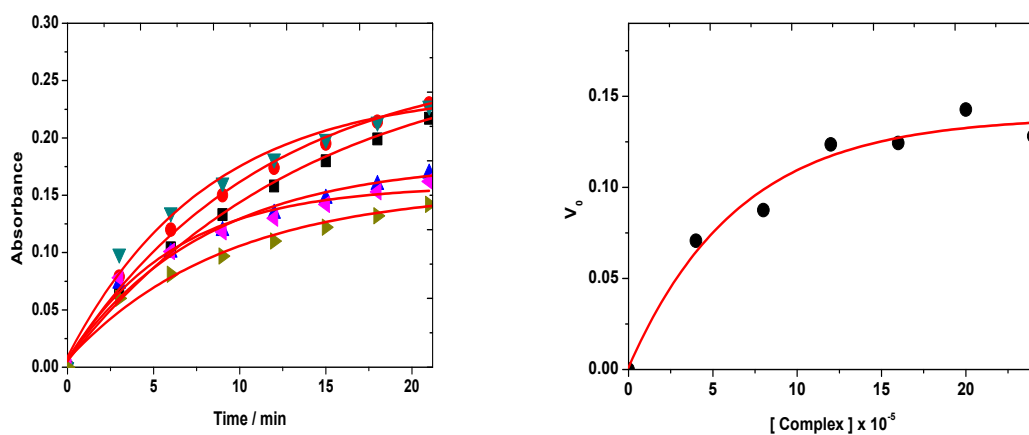


Fig 6. (left) relation between absorbance vs time at different concentrations of complex 1 with 4-*tert*-butylcatechol; (right) Oxidation rate of 4-*tert*-butylcatechol  $4 \times 10^{-2}$  M at different Concentrations of complex 1 in methanol,  $t = 25$  °C and wave length of 400 nm.

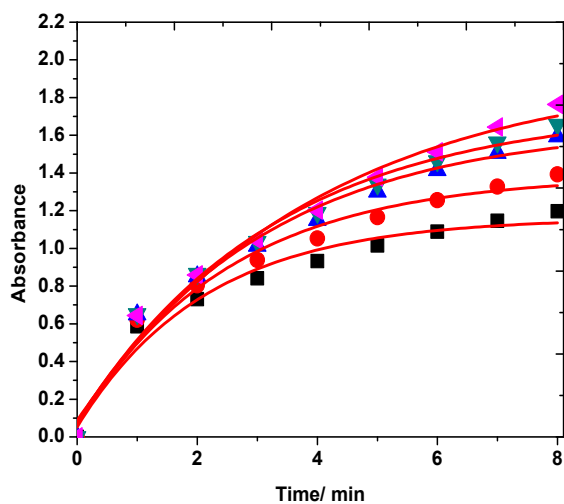


Fig 7. Oxidation of rate of 4-*tert*-butylcatechol ( $4 \times 10^{-2}$  M) at different Concentrations of  $\text{Et}_3\text{N}$  vs time; complex 1 =  $2 \times 10^{-4}$  M, methanol,  $t = 25$  °C and wave length of 400 nm.

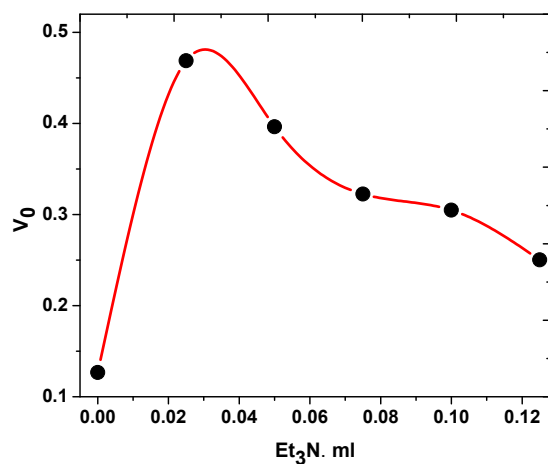


Fig 8. Dependence of rate of 4-*tert*-butylcatechol  $4 \times 10^{-2}$  M at different Concentrations of  $\text{Et}_3\text{N}$ ; complex 1 =  $2 \times 10^{-4}$  M, methanol,  $t = 25^\circ\text{C}$  and wave length of 400 nm.

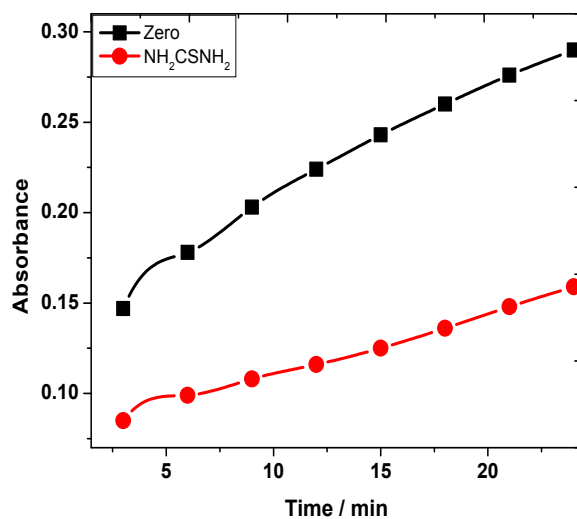


Fig 9. Oxidation of rate of 4-*tert*-butylcatechol 0.02 M at presence and absence of thiourea (TU) vs time; complex 1 =  $2 \times 10^{-4}$  M, methanol,  $t = 25^\circ\text{C}$  and wave length of 400 nm.

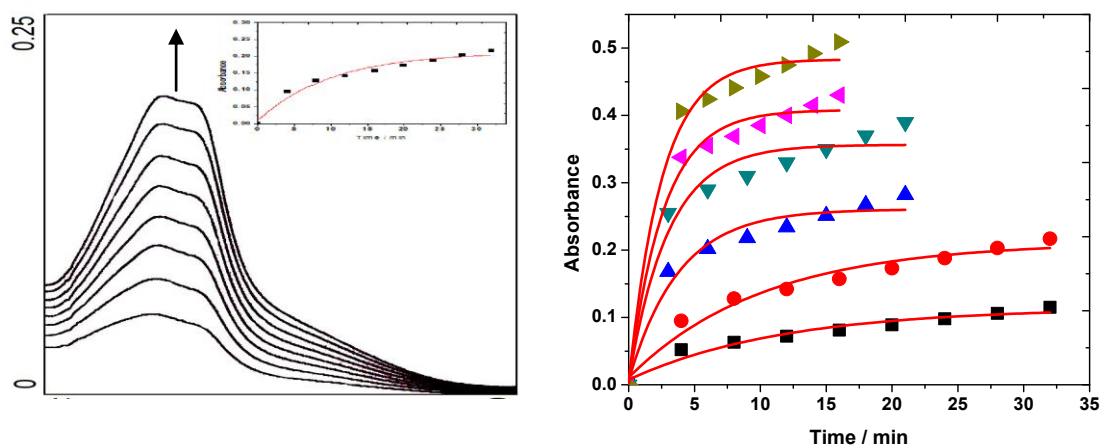


Fig 10. (Left) UV spectra changes of the reaction of complex 1 =  $2 \times 10^{-4}$  M with different concentrations of *o*-aminophenol in methanol; (right) relation between absorbance vs. time of the reaction at wave length of 400 nm.

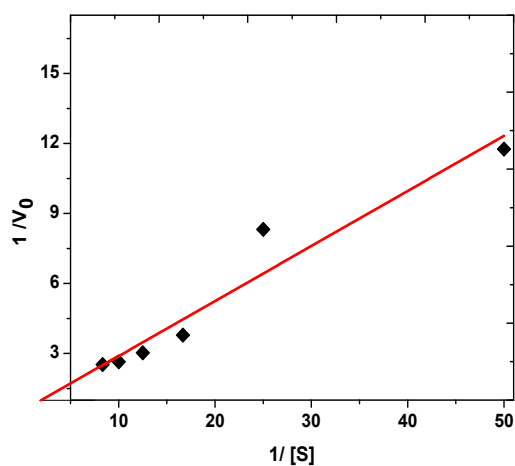


Fig 11. Lineweaver-Burk plot of  $1/V_0$  vs  $1/[S]$  concentrations with range 0.04 - 0.12 M for complex 1 for determining  $K_M$  and  $V_{max}$  values.

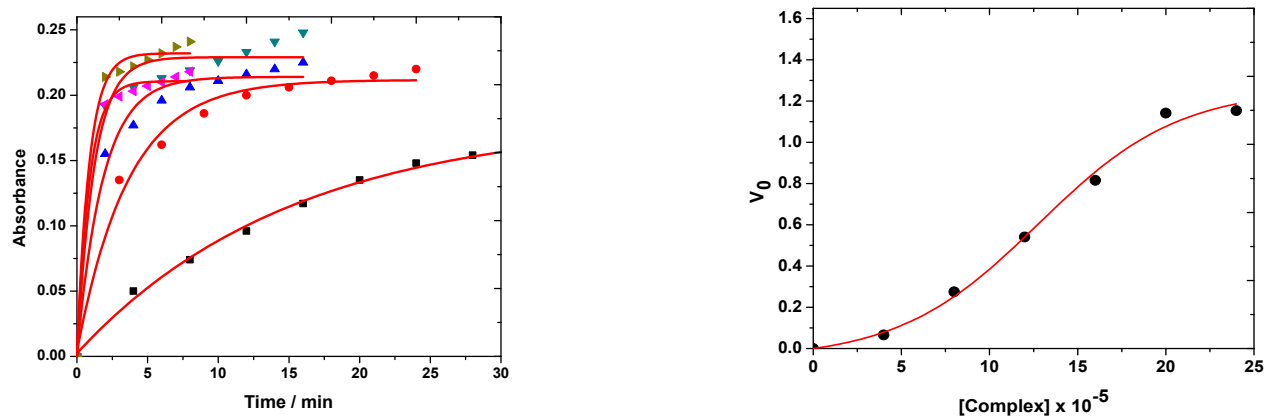


Fig 12. (left) relation between absorbance vs time at different concentrations of complex 1 with 4 *o*-aminophenol; (right) Oxidation rate of *o*-aminophenol  $4 \times 10^{-2}$  M at different Concentrations of complex 1 in methanol,  $t = 25$  °C and wave length of 400 nm.

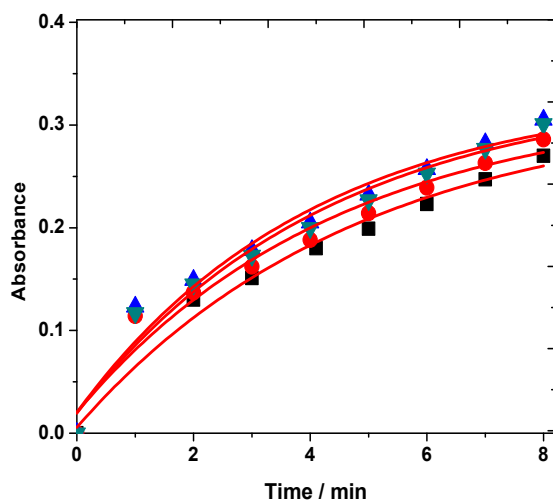
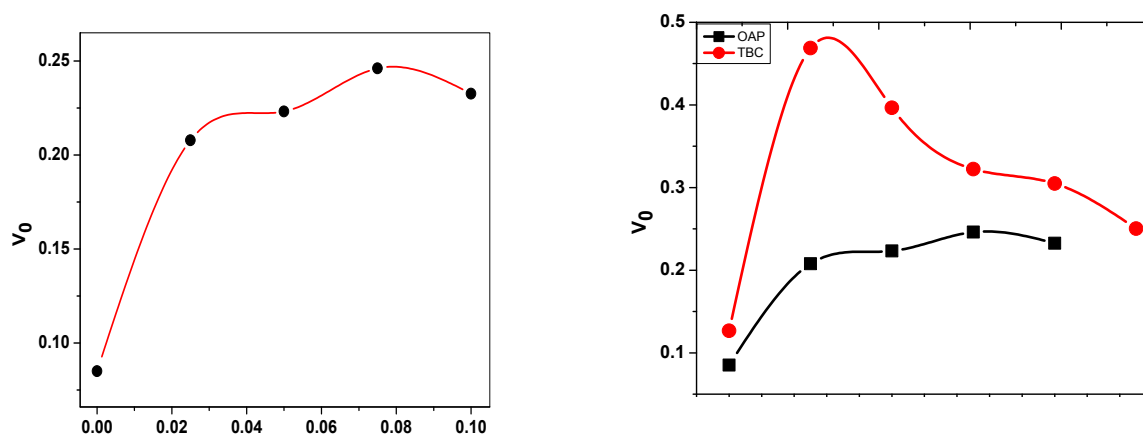


Fig 13. Oxidation of rate of *o*-aminophenol ( $2 \times 10^{-2}$  M) at different Concentrations of  $\text{Et}_3\text{N}$  vs time; complex 1 =  $2 \times 10^{-4}$  M, DMF,  $t = 25$  °C and wave length of 400 nm.



**Fig 14. Dependence of rate of *o*-aminophenol  $2 \times 10^{-2}$  M at different Concentrations of Et<sub>3</sub>N; complex 1 =  $2 \times 10^{-4}$  M, DMF,  $t = 25$  °C and wave length of 400 nm.**

### Conclusion:

Cobalt complexes as a catalyst for the oxidation reaction of 4-*tert*-butylcatechol (TBC) and 2-aminophenol (OAP) have been synthesized and completely characterized. The results clearly showed that both complexes act as catalysts for these reactions. The activity of both complexes was found to be dependent on the structure of ligand. The results also showed that the activity increase with the addition of Et<sub>3</sub>N and inhibited by the using of thiourea. Substrate and catalyst concentration dependence have been also studied and in both cases, saturation conditions have been reached.

### References

- Barry, C.E., Parmesh, G.N. and Begley, T.P. *Biochemistry*. **1989**, 28, 6323-33.  
 Eicken, C.; Zippel, F.; Büldt-Karentzopoulos, K.; Krebs, B. *FEBS Lett.* **1998**, 436, 293-299.  
 Frei, E. (1974) *Cancer Chemother. Rep.* 1987, 49-56.  
 Karlin, K.D. and Zubieta, J. *Copper Coordination Chemistry: Biochemical and Inorganic Perspective*. **1983**, Adenine Press, Guilderland, New York.  
 Kitajama, K.N. and Morooka, Y. *Chem. Rev.* **1994**, 94, 737-45.  
 Klabunde, T.; Eicken, C.; Sacchetti, J. C.; Krebs, B. *Nat. Struct. Biol.* **1998**, 5, 1084-1090.  
 Malmstrom, B. G. *Annu. Rev. Biochem.* **1982**, 51, 21-59.  
 Sheldon, R.A. and Kochi, J.K. *Metal - Catalysed Oxidation of Organic Compounds*, **1981**, Academic Press, New York.  
 Solomon, E. I.; Sundaram, U. M.; Machonkin, T. E. *Chem. Rev.* **1996**, 96, 2563-2605.  
 Toussaint, O. and Lerch, K. *Biochemistry*. **1987**, 26, 8567-71  
 VanHolde, K. E.; Miller, K. I. Hemocyanins. *Adv. Protein Chem.* **1995**, 47, 1-81.  
 Wilcox, D. E.; Porras, A. G.; Hwang, Y. T.; Lerch, K.; Winkler, M. E.; Solomon, E. I. *J. Am. Chem. Soc.* **1985**, 107, 4015-402.